Improving Ground Based Telescope Focus through Joint Parameter Estimation

Maj J. Chris Zingarelli
USAF AFIT/ENG

Lt Col Travis Blake
DARPA/TTO - Space Systems

Dr. Stephen Cain
USAF AFIT/ENG

Abstract-- Space Surveillance Telescope (SST) is a Defense Advanced Research Projects Agency (DARPA) program designed to facilitate the detection of space debris in earth's orbit. In order to achieve optimal performance, focusing of the telescope can be conducted by retrieving phase information in the image to determine the amount of defocus and then moving the mirrors axial to shift the focal point. One of its unique features is that operates with a mechanical shutter that's speed restricts the telescope to collecting long exposure imagery. Long exposure imagery $(\gg 10ms)$ consequently averages the atmosphere, which creates a point spread function (PSF) which can mimic one that contains fixed aberrations such as focus and spherical error. The average atmosphere masks the static aberrations of the telescope in the image affecting the ability to achieve an optimal focus. This paper will explore the joint estimation of the focus and the atmospheric seeing parameter. The Cramer-Rao lower bounds for variance are computed to facilitate an understanding of the joint estimation problem. These bounds will serve to demonstrate how the average atmospheric transfer function makes sensing a focus error more difficult in the presence of noise.

The views expressed are those of the author and do not reflect the official policy or position of the Department of Defense or the U.S. Government.

1. INTRODUCTION

The Department of Defense recently fielded an f/1 Mersenne-Schmidt telescope called the Space Surveillance Telescope (SST) that advances the United States space situational awareness (SSA) capability. SSA directly supports the stated US National Space Policy to "(p)reserve the Space Environment…the United States shall develop, maintain, and use space situational awareness information from commercial, civil, and national security sources to detect, identify, and attribute actions in space that are contrary to responsible use and the long-term sustainability of the space environment." **[1]**

The critical technology that enables SST's 6 deg^2 field of view (FOV) camera is its unique curved charged coupled device (CCD) shown in

Fig. 1. A high speed shutter was developed for the camera with a minimum exposure time of 25ms, considerably longer than the $1-10ms$ typically associated with a short exposure image **[2]**.

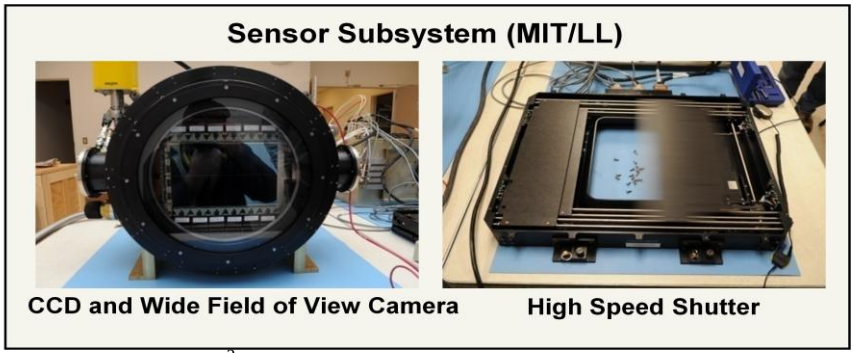

Fig. 1. SST's 6 deg^2 field of view camera and high speed mechanical shutter.

Report Documentation Page

Form Approved
OMB No. 0704-0188

1. REPORT DATE	2. REPORT TYPE	3. DATES COVERED
SEP 2012		**00-00-2012 to 00-00-2012**

4. TITLE AND SUBTITLE	5a. CONTRACT NUMBER
Improving Ground Based Telescope Focus through Joint Parameter Estimation	5b. GRANT NUMBER
	5c. PROGRAM ELEMENT NUMBER
6. AUTHOR(S)	5d. PROJECT NUMBER
	5e. TASK NUMBER
	5f. WORK UNIT NUMBER
7. PERFORMING ORGANIZATION NAME(S) AND ADDRESS(ES) **Air Force Institute of Technology ,USAF AFIT/ENG,2950 Hobson Way,Wright Patterson AFB,OH,45433**	8. PERFORMING ORGANIZATION REPORT NUMBER
9. SPONSORING/MONITORING AGENCY NAME(S) AND ADDRESS(ES)	10. SPONSOR/MONITOR'S ACRONYM(S)
	11. SPONSOR/MONITOR'S REPORT NUMBER(S)

12. DISTRIBUTION/AVAILABILITY STATEMENT
Approved for public release; distribution unlimited

13. SUPPLEMENTARY NOTES
In Advanced Maui Optical and Space Surveillance Technologies Conference (AMOS), 11-14 Sep 2012, Maui, HI.

14. ABSTRACT
Space Surveillance Telescope (SST) is a Defense Advanced Research Projects Agency (DARPA) program designed to facilitate the detection of space debris in earth?s orbit. In order to achieve optimal performance, focusing of the telescope can be conducted by retrieving phase information in the image to determine the amount of defocus and then moving the mirrors axial to shift the focal point. One of its unique features is that operates with a mechanical shutter that?s speed restricts the telescope to collecting long exposure imagery. Long exposure imagery  10ms consequently averages the atmosphere, which creates a point spread function (PSF) which can mimic one that contains fixed aberrations such as focus and spherical error. The average atmosphere masks the static aberrations of the telescope in the image affecting the ability to achieve an optimal focus. This paper will explore the joint estimation of the focus and the atmospheric seeing parameter. The Cramer-Rao lower bounds for variance are computed to facilitate an understanding of the joint estimation problem. These bounds will serve to demonstrate how the average atmospheric transfer function makes sensing a focus error more difficult in the presence of noise.

15. SUBJECT TERMS

16. SECURITY CLASSIFICATION OF:			17. LIMITATION OF ABSTRACT	18. NUMBER OF PAGES	19a. NAME OF RESPONSIBLE PERSON
a. REPORT **unclassified**	b. ABSTRACT **unclassified**	c. THIS PAGE **unclassified**	**Same as Report (SAR)**	**10**	

Currently, one of the main challenges to optimizing SSTs performance is to reduce the point spread function (PSF) through focus and alignment. The pixels in the CCD are $15\mu m$ however, the pixels canbe being 2x2 binned due to the expected atmospheric blurring. Fig. 2 shows the variations of full width half maximum (FWHM) blur spot in terms of $30\mu m$ binned pixels over 3 months.

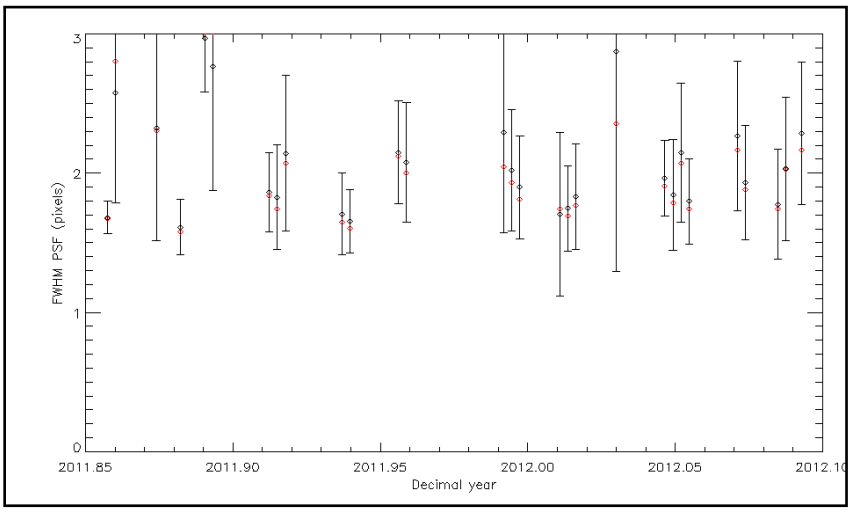

Fig. 2. Variations in the Full Width Half Maximum (FWHM) of SST's Point Spread Function (PSF) measured by 2x2 binned $15\mu m$ pixels.

Ideally, the PSF FWHM would be within one $30\mu m$ binned pixel. Reducing the PSF is possible by accurately determining the amount of focus error (and other aberrations) in the image of a calibration star then adjusting the focus and alignment to reduce the blur spot size. However due to the long exposures, to find unbiased estimates of the telescope aberrations from the star image the atmospheric effects must be included in the telescope model.

2. TELESCOPE MODEL

The telescope model developed in this section follows a similar model employed for analysis of the Hubble Space Telescope **[3]**. The telescope is considered a linear shift invariant system where the impulse response of the system will be the PSF. The light propagating from the distance point source (i.e. a star) is assumed to be temporally incoherent. Therefore, according to Goodman, the image irradiance in the x detector plane, $i(x)$, is the convolution of point source irradiance, $\delta(x)$, with telescopes PSF **[4]**. The parameters used in the telescope model are listed in Tab. 1.

Tab. 1. Telescope Parameters

Model Parameter	Value
Center Wavelength	500nm
Telescope Pupil/Obscuration Diameter	3.5m/1.8m
Telescope Effective Focal Length	3.5m
CCD Pixel Pitch	15µm
Star Irradiance per Frame	~10^4 photons
Background Irradiance per Frame	300 photons
Grid Size	2^11

The pupil function, $A(u,v)$, of the telescope is defined by its annular aperture shown in Fig. 3a, where u and v are coordinates in the pupil plane. Wave front error caused by defocus is introduced into the pupil function using the Zernike polynomial for defocus, **[5]**

$$\varphi_4(u,v) = 3.464(u^2+v^2) - 1.732. \quad (1)$$

The amount of focus error is captured by scaling $\varphi_4(u,v)$ with a Zernike coefficient for defocus, Z_4

$$error(u,v) = Z_4\varphi_4(u,v). \tag{2}$$

An image of $\varphi_4(u,v)$ scaled by a 25 wave coefficient is shown in Fig. 3b. The aberrations are then represented in the pupil plane, u_1, by the generalized pupil function

$$\mathcal{P}(u_1) = A(u_1)\exp\left[\, j \cdot error(u_1)\right]. \tag{3}$$

The PSF is then computed as

$$\begin{aligned} h_{opt}(m) &= \left|\sum_{u_1}\mathcal{P}(u_1)e^{j2\pi mu_1}\right|^2 \\ &= \sum_{u_1}\mathcal{P}(u_1)e^{j2\pi mu_1}\sum_{u_2}\mathcal{P}(u_2)e^{-j2\pi mu_2}. \\ &= \sum_{u_1}A(u_1)e^{jZ_4\phi_4(u_1)}e^{j2\pi mu_1}\sum_{u_2}A(u_2)e^{-jZ_4\phi_4(u_2)}e^{-j2\pi mu_2} \\ &= \left|H(m)\right|^2 = H(m)H(m)^*, \end{aligned} \tag{4}$$

where, H is the field in the detector plane **[4]**. The telescope's PSF with 25 waves of defocus is shown in Fig. 3c where m is a pixel coordinate in the x detector plane. The large amount of defocus causes the PSF to have an annular shape.

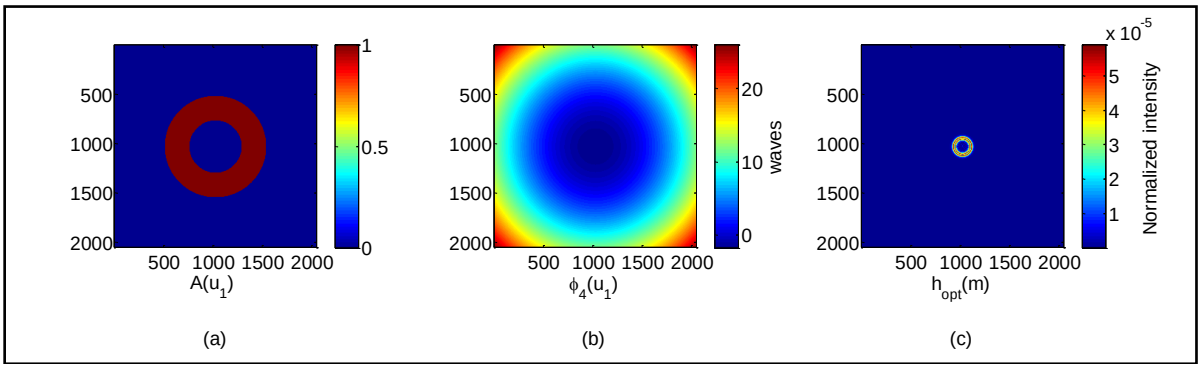

Fig. 3. (a) Pupil function used to model SST (b) Zernike polynomial for defocus with $Z_4 = 25$ waves (c) Telescopes PSF with $Z_4 = 25$ waves of focus error

For a more complete model telescope model, the effect of the finite square pixels, $a = 15\mu m,$ is included in the PSF where the transfer function for the pixels and telescope respectively are represents as the following digital Fourier transforms, $\mathcal{F}$,

$$\mathcal{H}_{pixel}(u_1) = \mathcal{F}\{rect(ax)\}, \text{ and} \tag{5}$$

$$\mathcal{H}_{opt}(u_1) = \mathcal{F}\{h_{opt}(m)\}, \text{ therefore} \tag{6}$$

$$h_{telescope}(m) = \mathcal{F}^{-1}\{\mathcal{H}_{opt}(u_1)\mathcal{H}_{pixel}(u_1)\}. \tag{7}$$

Images observed by SST have been measured to be shot noise dominated, so the image data, $d(m),$ is considered to be Poisson and has a mean value that is equal to the irradiance of light in that pixel **[2]**

$$E\left[d\left(m\right)\right]=i(m). \tag{8}$$

The model for the image irradiance centered on the optical axis is

$$i_{telescope}(m)=\sum_{x}\theta_1\delta(x)h_{telescope}(m-x)+B. \tag{9}$$

It includes additional terms to account for the background light, B, and the total photons emitted from the star per integration time, θ_1. The joint distribution of the image data is represented by the Poisson probability mass function,

$$\prod^{m}P[d(m)]=\prod^{m}\frac{e^{-i_{telescope}(m)}i_{telescope}(m)^{d(m)}}{d(m)!}, \tag{10}$$

the associated log likelihood equation is

$$\begin{aligned}L\left(Z_4\right)&=\ln\left(\prod^{m}P\left[d(m)\right]\right)\\&=\sum_{m}\left\{-i_{telescope}(m)+d(m)\ln i_{telescope}(m)-\ln d(m)!\right\}.\end{aligned} \tag{11}$$

3. CRAMER-RAO LOWER BOUND (CRLB) FOR VARIANCE

The Cramer-Rao lower bounds provides a theoretical lower limit of variance for estimates of the Zernike coefficient for defocus, $\hat{Z}_4$ [3]. The bounds in Fig. 5 illustrate that standard deviations of $\hat{Z}_4$ on the order of 10^{-1} waves are possible even in the presence of long exposure atmosphere. To determine the CRLB for estimates of the Zernike coefficient for defocus the Fisher information, $J(Z_4)$, is computed via the following calculation [6]

$$J(Z_4)=-E\left[\frac{\partial^2 L\left(Z_4\right)}{\partial {Z_4}^2}\right], \tag{12}$$

where, the CRLB for the variance of $\hat{Z}_4$ is defined as

$$\mathrm{var}(\hat{Z}_4)\geq J\left(Z_4\right)^{-1}. \tag{13}$$

The first and second derivative of the log likelihood function Eq. (11) respectively are

$$\frac{\partial L\left(Z_4\right)}{\partial Z_4}=\sum_{m}\left(\frac{d\left(m\right)\theta_1}{i_{telescope}(m)}-\theta_1\right)\frac{\partial h_{telescope}\left(m\right)}{\partial Z_4}, \text{ and} \tag{14}$$

$$\frac{\partial^2 L\left(Z_4\right)}{\partial {Z_4}^2}=\sum_{m}\left(\frac{d\left(m\right)\theta_1}{i_{telescope}(m)}-\theta_1\right)\frac{\partial^2 h_{telescope}\left(m\right)}{\partial Z_4^2}-\frac{d\left(m\right)\theta_1}{{i_{telescope}}^2(m)}\left(\frac{\partial h_{telescope}\left(m\right)}{\partial Z_4}\right)^2. \tag{15}$$

The resulting Fisher information is

$$J\left(Z_4\right)=-E\left[\frac{\partial^2 L\left(Z_4\right)}{\partial {Z_4}^2}\right]=\sum_{m}\left(\frac{\theta_1}{i_{telescope}}\right)\left(\frac{\partial h_{telescope}(m)}{\partial Z_4}\right)^2. \tag{16}$$

The derivative of the PSF with respect defocus is

$$\frac{\partial h_{telescope}(m)}{\partial Z_4} = \left[\frac{\partial H^*}{\partial Z_4}H + \frac{\partial H}{\partial Z_4}H^*\right] \otimes \mathcal{F}^{-1}\left\{\mathcal{H}_{pixel}(u_1)\right\}. \tag{17}$$

The derivative of the wavefront in the detector plane with respect to (w.r.t) Z_4 is

$$\begin{aligned}\frac{\partial H}{\partial Z_4} &= j\sum_{u_1}\phi_4(u_1)A(u_1)e^{jZ_4\phi_4(u_1)}e^{j2\pi m u_1} \\ &= j\mathcal{F}\left\{\phi_4(u_1)A(u_1)e^{jZ_4\phi_4(u_1)}\right\}.\end{aligned} \tag{18}$$

Thus, recalling that for arbitrary variables a and b; $j\left[(a+jb)-(a-jb)\right] = -2b = -2\,\mathrm{Im}(a+jb)$ leading to the first derivative of the PSF to be

$$\begin{aligned}\frac{\partial h_{telescope}(m)}{\partial Z_4} &= j\left[-\mathcal{F}\left\{\phi_4(u_1)A(u_1)e^{jZ_4\phi_4(u_1)}\right\}H + \mathcal{F}\left\{\phi_4(u_2)A(u_2)e^{jZ_4\phi_4(u_2)}\right\}H^*\right] \\ &\otimes \mathcal{F}^{-1}\left\{\mathcal{H}_{pixel}(u_1)\right\} \\ &= -2\,\mathrm{Im}\left[\mathcal{F}\left[\phi_4(u_2)A(u_2)e^{jZ_4\phi_4(u_2)}\right]H^*\right] \otimes \mathcal{F}^{-1}\left\{\mathcal{H}_{pixel}(u_1)\right\}.\end{aligned} \tag{19}$$

The resulting Fisher information for the optical system containing focus error is

$$J(Z_4) = 4\sum_m\left(\frac{\theta_1}{i_{Z_4}}\right)\left\{\mathrm{Im}\left[\mathcal{F}\left[\phi_4(u_2)A(u_2)e^{jZ_4\phi_4(u_2)}\right]H^*\right] \otimes \mathcal{F}^{-1}\left\{\mathcal{H}_{pixel}\right\}\right\}^2 \tag{20}$$

where $J(Z_4)^{-1}$ is plotted as the purple line with star data markers in Fig. 5.

Because SST uses a shutter, with an integration time greater than 25ms, an accepted model for that atmosphere is a long-exposure atmospheric transfer function, which given by Goodman as **[4]**

$$\mathcal{H}_{atm}(u_1) = \exp\left\{-3.44\left(\frac{\bar{\lambda} f u_1}{r_0}\right)^{5/3}\right\}. \tag{21}$$

In Eq. (21) $\bar{\lambda}$ is the mean wavelength, f is the telescope focal length, and r_0 is the atmospheric seeing parameter. The total PSF is then computed as

$$h_{total}(m) = \mathcal{F}^{-1}\left\{\mathcal{H}_{opt}(u_1)\mathcal{H}_{pixel}(u_1)\mathcal{H}_{atm}(u_1)\right\}. \tag{22}$$

Samples of the three transfer functions are shown in Fig. 4 (a-c) to illustrate how the pixels and atmosphere reduce special frequency content of the diffraction limited telescope's optical transfer function and due to it Fourier transform relationship broaden the PSF. The x-axis is shown in terms of the spatial frequency, u_1, divided by the cutoff frequency, u_0, for the annular telescope pupil function. As the focus error increases $\mathcal{H}_{opt}(u_1)$ begins to increasingly limit the spatial resolution of the telescope further broadening the PSF.

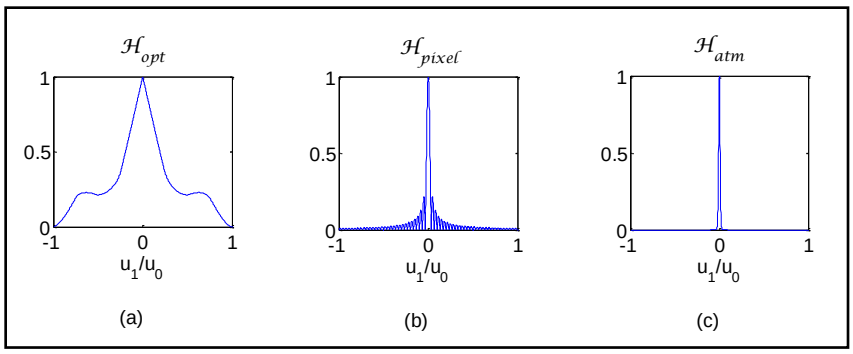

Fig. 4. (a) Telescope Models Optical Transfer Function (OTF) with $Z_4 = 0$ (b) $15\mu m$ Pixels Transfer Function (c) Atmospheric Transfer Function with $r_0 = 8cm$

By including the effects of the atmosphere in the PSF, the image intensity model in Eq. (9) becomes

$$i_{total}(m) = \sum_x \theta_1 \delta(x) h_{total}(m-x) + B. \tag{23}$$

The elements of the Fisher information matrix,

$$I = \begin{bmatrix} J(Z_4) & J(Z_4, r_0) \\ J(Z_4, r_0) & J(r_0) \end{bmatrix} \tag{24}$$

are calculated in order to determine the CRLB for variance of $\hat{Z}_4$ in the presence of an average atmosphere. Using the log likelihood function in Eq. (11) and taking the second derivative of Eq. (14) w.r.t r_0 & Z_4

$$\frac{\partial^2 L(Z_4, r_0)}{\partial Z_4 \partial r_0} = \sum_m \left(\frac{d(m)\theta_1}{i_{total}(m)} - \theta_1 \right) \frac{\partial^2 h_{total}(m)}{\partial Z_4 \partial r_0} - \frac{d(m)\theta_1}{i_{total}^{\ 2}(m)} \left(\frac{\partial h_{total}(m)}{\partial Z_4} \right) \left(\frac{\partial h_{total}(m)}{\partial r_0} \right), \tag{25}$$

$$\frac{\partial^2 L(Z_4, r_0)}{\partial r_0^{\ 2}} = \sum_m \left(\frac{d(m)\theta_1}{i_{total}(m)} - \theta_1 \right) \frac{\partial^2 h_{total}(m)}{\partial r_0^{\ 2}} - \frac{d(m)\theta_1}{i_{total}^{\ 2}(m)} \left(\frac{\partial h_{total}(m)}{\partial r_0} \right)^2, \text{ and} \tag{26}$$

$$\frac{\partial^2 L(Z_4, r_0)}{\partial Z_4^{\ 2}} = \sum_m \left(\frac{d(m)\theta_1}{i_{total}(m)} - \theta_1 \right) \frac{\partial^2 h_{total}(m)}{\partial Z_4^{\ 2}} - \frac{d(m)\theta_1}{i_{total}^{\ 2}(m)} \left(\frac{\partial h_{total}(m)}{\partial Z_4^2} \right). \tag{27}$$

Because $E[d(m)] = i_{total}(m)$ the elements of the Fisher information matrix are

$$J(Z_4, r_0) = -E\left[\frac{\partial^2 L(Z_4, r_0)}{\partial Z_4 \partial r_0} \right] = \sum_m \left(\frac{\theta_1}{i_{total}} \right) \left(\frac{\partial h_{total}(m)}{\partial z_4} \right) \left(\frac{\partial h_{total}(m)}{\partial r_0} \right), \tag{28}$$

$$J(r_0) = -E\left[\frac{\partial^2 L(Z_4)}{\partial r_0^{\ 2}} \right] = \sum_m \left(\frac{\theta_1}{i_{total}} \right) \left(\frac{\partial h_{total}(m)}{\partial r_0} \right)^2, \text{ and} \tag{29}$$

$$J(Z_4) = -E\left[\frac{\partial^2 L(Z_4)}{\partial Z_4^{\ 2}} \right] = \sum_m \left(\frac{\theta_1}{i_{total}} \right) \left(\frac{\partial h_{total}(m)}{\partial z_4} \right)^2. \tag{30}$$

Then the derivatives of the PSF are

$$\frac{\partial h_{total}(m)}{\partial Z_4} = \mathcal{F}^{-1}\left\{\mathcal{F}\left[\frac{\partial H^*}{\partial Z_4}H + \frac{\partial H}{\partial Z_4}H^*\right]\mathcal{H}_{atm}\mathcal{H}_{pixel}\right\}$$

$$= \mathcal{F}^{-1}\left\{\mathcal{F}\left\{-2\,\mathrm{Im}\left[\mathcal{F}\left[\phi_4(u_2)A(u_2)e^{jZ_4\phi_4(u_2)}\right]H^*\right]\right\}\mathcal{H}_{atm}\mathcal{H}_{pixel}\right\}, \text{ and} \tag{31}$$

$$\frac{\partial h_{total}(m)}{\partial r_0} = \frac{5.73}{r_0^{8/3}}\mathcal{F}^{-1}\left\{\mathcal{H}_{opt}u_3^{5/3}\mathcal{H}_{pixel}\mathcal{H}_{atm}\right\}.$$

The CRLB for variance is computed by inverting the Fisher information matrix

$$\begin{bmatrix} \mathrm{var}(\hat{Z}_4) & \mathrm{cov}(\hat{Z}_4, r_0) \\ \mathrm{cov}(\hat{Z}_4, r_0) & \mathrm{var}(r_0) \end{bmatrix} \geq I^{-1}. \tag{32}$$

The resulting CRLB for the standard deviation, CRLB σ , of $\hat{Z}_4$ is plotted in Fig. 5 for cases with and without an average atmosphere present. Atmospheric turbulence increases CRLB σ and as r_0 decrease the effect of the atmosphere on the bound increase. In addition as Z_4 decrease the lower bound increases. Therefore, estimation of Z_4 should become more inaccurate as the amount of defocus decreases. In addition, as r_0 decreases the CRLB σ uniformly increases indicating that more turbulent atmospheres will increase the variance on estimates of defocus.

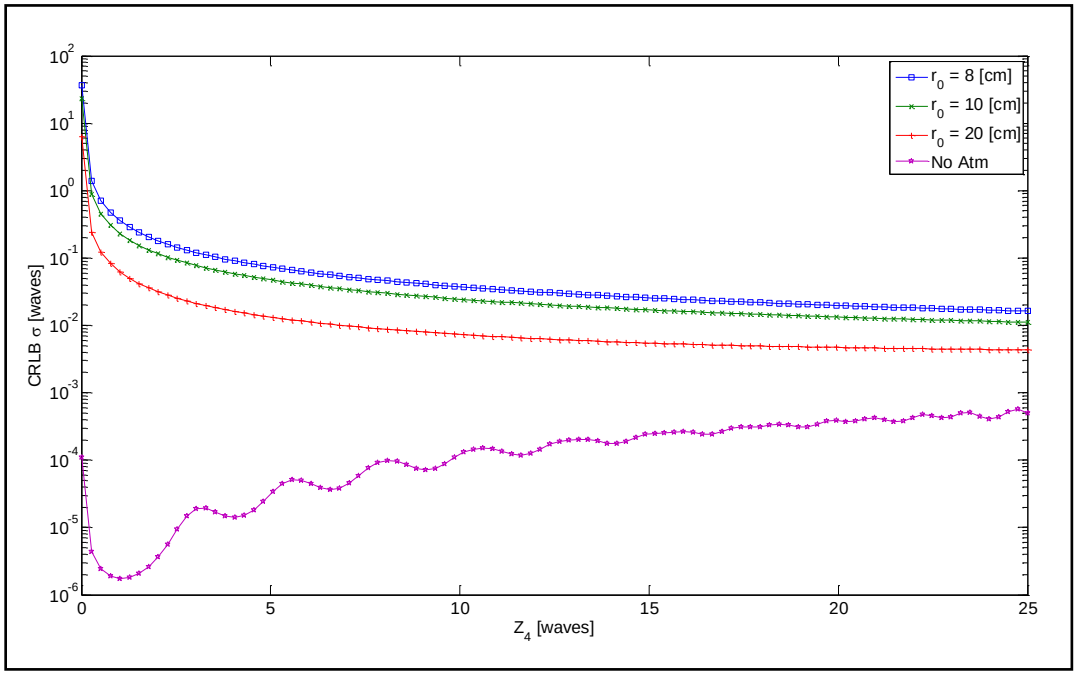

Fig. 5**.** Cramer-Rao Lower Bound of the standard deviation, CRLB σ, of estimates for the defocus parameter, $\hat{Z}_4$. CRLB σ are shown for cases with no atmosphere in the model and increasing atmospheric seeing by changing r_0.

4. STAR SIMULATIONS

Stars were simulated as system impulses, $\delta(x)$, and then the effects of the atmosphere, telescope, defocus, pixilation, background light and star intensity were introduced using Eq. (23). The analog images of a star with and without atmospheric effects are shown in Fig. 6. (a) & (b). The pixilated images of those same stars are picture in Fig. 6. (c) & (d). Shot noise is simulated in the stars using a Poisson random number generator the training data, $d(m)$, evaluate the performance of the estimators describes in Sec. 8.

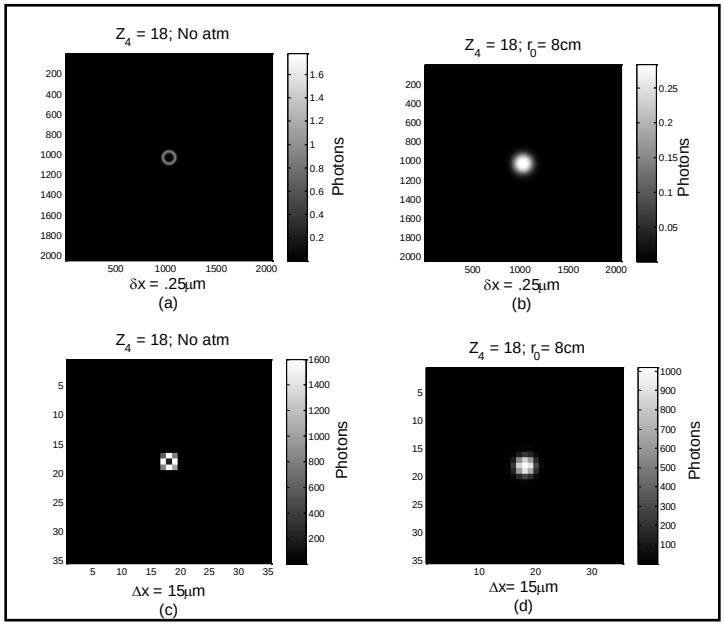

Fig. 6. (a) Simulated analogue image of a star with $Z_4 = 18$ waves and no atmosphere. (b) Simulated analog image of a star with $Z_4 = 18$ waves and an average atmosphere where $r_0 = 8cm$. (c) Simulated digital image of a star with $Z_4 = 18$ waves and no atmosphere. (d) Simulated digital image of a star with $Z_4 = 18$ waves and an average atmosphere where $r_0 = 8cm$.

5. PARAMETER ESTIMATION

The method of least squares (LS) estimation was used to estimate the Zernike coefficient for defocus, $\hat{Z}_4$ from the simulated star data. The LS method is used because of computer precision challenges encountered in the maximum likelihood estimation approach due to the large background noise levels inside the log-likelihood function. In addition, the LS method does not require any parametric assumptions making the estimator more robust to changes in the noise statistics **[5]**. The intensity models from Eqs. (9) & (23) are used to define the sum of squares

$$Q_{telescope} = \sum_x \left(i_{telescope}(m) - \sum_x \theta_1 \delta(x) h_{telescope}(x-m) - B \right)^2, \text{ and} \tag{33}$$

$$Q_{total} = \sum_x \left(i_{total}(m) - \sum_x \theta_1 \delta(x) h_{total}(x-m) - B \right)^2. \tag{34}$$

In order to estimate defocus, the unknown photons per image, θ_1, must also be estimated from the data by take the derivative of Eq. (33) and (34) and setting them equal to zero to get the generalized function

$$\theta_1 = \frac{\sum_x \left[i(m) - B \right] h(m)}{\sum_x h^2(m)} \tag{35}$$

Determining $\hat{Z}_4$ without accounting for the atmosphere is found by the single parameter estimate

$$\hat{Z}_4 = \arg\min_{Z_4} \left(Q_{telescope} \right), \tag{36}$$

or by accounting for the atmosphere with the joint estimator

$$\begin{bmatrix} \hat{Z}_4 \\ \hat{r}_0 \end{bmatrix} = \arg\min_{Z_4, r_0} \left(Q_{total} \right). \tag{37}$$

By conducting a numerical grid search of realistic values for Z_4 the parameter estimates that the gives the LS solutions are numerically determined. Finding $\hat{Z}_4$ for multiple image frames of simulated star data the results are used to determine the sample mean and variance for the LS estimator.

To produce the plot in Fig. 7a, training data, $d(m)$, is generated without shot noise and with focus errors ranging from 3-24 waves in order to determine the estimators biases. Estimates of defocus using Eq. (36) are made on simulated stars with and without an average atmosphere present. The graph shows that when the simulated star data has an average atmosphere, the single parameter estimator has a defocus dependent bias. In contrast, the results of joint estimator, Eq. (37), on the same simulated star data with an average atmosphere present does not have a significant bias.

The joint estimator is used to estimate the defocus from training data containing shot noise with the mean and standard deviation plotted in Fig. 7b. As the amount of defocus decreases the standard deviation increases significantly due to the narrowing of the PSF. As the blur spot narrows less of the shape of the PSF can be discerned from the star images affecting the accuracy of the estimates of Z_4. The sample standard deviation, σ_s, of the joint parameter estimate also plotted with their associated CRLB σ in Fig. 7c. The CRLB σ is not achieved by σ_s but, the standard deviation is below a wave until the blur spot becomes too small.

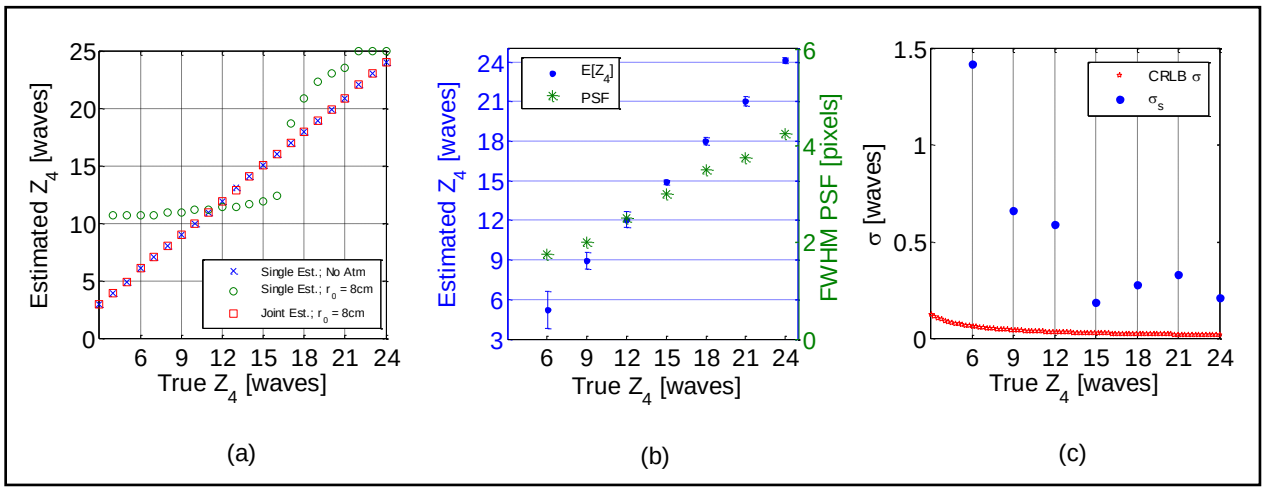

Fig. 7 (a) The estimated defocus parameter is determined from simulated star data with no noise present. The blue X marks the single parameter estimate for defocus without an atmosphere present in the simulated star data. The green circles are the single parameter estimates of Z_4 where $r_0 = 8cm$ in the simulated star data. The red boxes are the joint parameter estimate of Z_4 where $r_0 = 8cm$ in the simulated star data. (b) The joint parameter estimates from the simulated stars with shot noise $E\left[\hat{Z}_4\right]$ and σ_s are represented as blue dots and plotted as a function of the defocus. The FWHM of the PSFs are plotted with the green asterisks as a function of defocus. (c) The joint parameter estimates σ_s are plotted as blue dots and the CRLB σ as red stars as a function of star defocus.

6. CONCLUSIONS

The fact that the atmosphere can affect estimation of the coefficient for the defocus polynomial demonstrates the need to account for the effects atmosphere seeing in order to accurately estimate SSTs aberrations from star images. Joint estimation of the atmospheric seeing parameter for the long exposure atmosphere $(\gg 10ms)$ and the coefficient for the defocus polynomial demonstrates an effective way to account for the atmosphere when estimating aberrations from imagery data. Results of this work are promising in that there is no indication thus far that joint estimation of the Zernike coefficients for the static aberrations in SST can't be determined and/or alleviated.

7. FUTURE WORK

The next steps in this research will be to expand the joint estimator to include the other aberrations present in SST data. In addition, laboratory experiments can be conducted by imaging point sources in a diffraction limited telescope then defocusing the telescope and adding atmospheric turbulence to further show that the algorithms developed for joint estimations of Z_4 work. Ultimate validation of the work will be to sharpen the SST camera images by reducing the aberrations in the telescope using the basic techniques developed herein.

8. ACKNOLEGMENTS

This material is based upon work sponsored by DARPA. In addition, MIT Lincoln Laboratory inputs were instrumental in problem identification. MIT also provided the SST sensor subsystem images and PSF chart in Sec. 1.

9. WORKS CITED

[1] U. S. Govnernment, "NATIONAL SPACE POLICY of the UNITED STATES of AMERICA," United States Govnernment, Washington DC, 2010.

[2] J. W. Goodman, Statistical Optics, New York: Wiley Interscience, 1985.

[3] J. M. J. S. T. a. S. J. Fienup, "Hubble Space Telescope characterized by using phase-retrieval algorithms," *Applied Optics,* vol. 32, no. 10, p. 17471767, 1993.

[4] J. W. Goodman, Fourier Optics, Greenwood Village, CO: Roberts & Company, 2005.

[5] R. Noll, "Zernike polynomials and atmospheric turbulence," *J. Opt. Soc. Am.,* vol. 66, pp. 207-211, 1976.

[6] S. M. Kay, Fundamentals of Statistical Signal Processing, Upper Saddle River, NJ: Prentice-Hall, 2011.

[7] P. H. Kvam and B. Vidakovis, Nonparametic Statistics with Apllications to Science and Engineering, Hoboken: John Wiley & Sons, Inc, 2007.